Effects of the 3d transition metal doping on the structural, electronic, and magnetic properties of BeO nanotubes*

Zhang Jian-Min(张建民)[a)†], Song Wan-Ting(宋婉婷)[a)], Li Huan-Huan(李欢欢)[a)], Xu Ke-Wei(徐可为)[b)], and Ji Vincent[c)]

[a)] College of Physics and Information Technology, Shaanxi Normal University, Xi'an 710062, China
[b)] State Key Laboratory for Mechanical Behavior of Materials, Xi'an Jiaotong University, Xi'an 710049, China
[c)] ICMMO/LEMHE, Université Paris-Sud 11, 91405 Orsay Cedex, France

(Received 24 April 2013; revised manuscript received 2 July 2013; published 3 December 2013)

First-principles calculations have been performed on the structural, electronic, and magnetic properties of seven 3d transition-metal (TM) impurities (V, Cr, Mn, Fe, Co, Ni, and Cu) doped armchair (5,5) and zigzag (8,0) beryllium oxide nanotubes (BeONTs). The results show that there exists a structural distortion around the 3d TM impurities with respect to the pristine BeONTs. The magnetic moment increases for V- and Cr-doped BeONTs and reaches a maximum for Mn-doped BeONT, and then decreases for Fe-, Co-, Ni-, and Cu-doped BeONTs successively, consistent with the predicted trend of Hund's rule to maximize the magnetic moments of the doped TM ions. However, the values of the magnetic moments are smaller than the predicted values of Hund's rule due to the strong hybridization between the 2p orbitals of the near O and Be ions of BeONTs and the 3d orbitals of the TM ions. Furthermore, the V-, Co-, and Ni-doped (5,5) and (8,0) BeONTs with half-metal ferromagnetism and thus 100% spin polarization character are good candidates for spintronic applications.

Keywords: BeO nanotubes, transition-metal atoms, half-metal ferromagnets, first-principles calculation

PACS: 71.15.Mb, 71.20.Be, 73.22.–f, 73.63.Fg **DOI:** 10.1088/1674-1056/23/1/017103

1. Introduction

In the past few decades, half-metal ferromagnets (HMFs), which have only one spin channel for conduction at the Fermi level, have attracted increasing research interest because of their potential applications in spintronics. HMFs were first discovered by de Groot *et al.* in Heusler compounds in 1983.[1] After that, some HMFs have also been predicted theoretically or confirmed experimentally in ferromagnetic metallic oxides,[2–4] in Heusler and half-Heusler compounds,[5–10] and in dilute magnetic semiconductors (DMSs).[11–13] Though many HMFs have been reported, it is still very important to find new HMFs, especially nanoscale HMF materials, because magnetic nanostructures are a scientifically interesting and technologically important area of research with many current and future applications in permanent magnetism, magnetic recording, and spintronics.

BeO nanotubes (BeONTs) are of great importance due to their high thermal and mechanical stability. Models of pristine BeONTs were proposed, and their structural, cohesion, and electronic properties were predicted.[13,14] It is found that these nanotubes are wide-band-gap dielectrics with very small helicity-induced differences in the gaps. In addition, the BeONTs adopt interesting mechanical properties, namely, their Young's moduli are comparable with those of carbon nanotubes. The BeONTs would be a wonderful candidate for the host materials of half-metal ferromagnets.

In this paper, the structural, electronic, and magnetic properties of seven 3d transition-metal (TM) (V, Cr, Mn, Fe, Co, Ni, Cu) doped armchair (5,5) and zigzag (8,0) BeONTs are investigated using the projector-augmented-wave (PAW) potential within the generalized-gradient approximation (GGA). The rest of the paper is organized as follows. Section 2 gives the calculation method. In Section 3, we present the doped configurations and the corresponding electronic and magnetic properties. Finally, the conclusions of the work are given in Section 4.

2. Calculation method

The calculations are performed within the framework of density functional theory (DFT) using the PAW potential and a plane-wave basis set, as implemented in VASP.[15–19] The electron exchange and correlation are treated by using the Perdew–Burke–Ernzerhof (PBE) formulation of the GGA.[20] The models of (5,5) and (8,0) BeONTs are constructed in periodical tetragonal supercells with lattice constants of about $a = b = 18.5$ Å and $a = b = 17.8$ Å, respectively. The $2s^2 2p^4$ and $2s^2$ electrons are taken as the valence electrons of the O and Be atoms, respectively. To minimize the interaction be-

*Project supported by the National Basic Research Program of China (Grant No. 2010CB631002) and the National Natural Science Foundation of China (Grant Nos. 51071098, 11104175, and 11214216).

†Corresponding author. E-mail: jianm_zhang@yahoo.com

© 2014 Chinese Physical Society and IOP Publishing Ltd

tween two adjacent TM atoms, the lattice constant c along the tube axis is taken to be four and two times the periodic length for the armchair (5,5) and zigzag (8,0) BeONTs, respectively. The Brillouin zone integration is performed by using the Gamma centered Monkhorst–Pack scheme[21] with $1\times1\times11$ k points. To avoid the numerical instability due to level crossing and quasi-degeneracy near the Fermi level, we use the first-order Methfessel–Paxton method with a width of 0.2 eV. In order to find the ground geometries of the doped systems, the conjugate-gradient (CG) minimization scheme is utilized. The optimization will continue until the convergence tolerance of the total energies of the last two sequential steps is less than 10^{-4} eV/atom and the maximum force on each atom is less than 0.02 eV/Å.

3. Results and discussion

We first optimize the structures of pristine armchair (5,5) and zigzag (8,0) BeONTs. The calculated average Be–O bond lengths of (5,5) and (8,0) BeONTs are about 1.615 Å and 1.660 Å, respectively. In detail, the Be atoms move inward towards the tube axis, while the O atoms move in the opposite direction. Thus, the relaxed armchair (5,5) and zigzag (8,0) BeONTs can be characterized by two coaxial cylindrical tubes with an outer O cylinder (in diameter of 6.992 Å for the (5,5) tube and 6.778 Å for the (8,0) tube) and an inner Be cylinder (in diameter of 6.855 Å for the (5,5) tube and 6.632 Å for the (8,0) tube), resulting in a radial buckling of 0.137 Å for the (5,5) tube and 0.146 Å for the (8,0) tube. Similar radial buckling phenomena between cations and anions were also observed in SiCNTs and BNNTs.[22,23] Figures 1(a) and 1(b) display the structure models of the 3d TM (V, Cr, Mn, Fe, Co, Ni, Cu) doped (5,5) and (8,0) BeONTs, respectively, in which the blue, yellow, and gray balls denote O, Be, and TM atoms, respectively. The blue balls marked with white numbers 1, 2, and 3 denote the three nearest-neighbor O atoms of the TM impurity.

In order to avoid the interaction between adjacent 3d TM atoms, the lattice constant c along the tube axis is taken to be four and two times the periodic length for the armchair (5,5) and zigzag (8,0) BeONTs, respectively. $Be_{39}(TM)O_{40}$ and $Be_{31}(TM)O_{32}$ correspond to 1.25 at.% and 1.56 at.% of 3d TM impurities in (5,5) and (8,0) BeONTs, respectively. The optimized local bond lengths around the substitutional 3d TM impurity, including the bond lengths between the TM atom and its three nearest-neighbor O atoms (d_{TM-O}) as well as the ranges of bond lengths between the three nearest-neighbor O atoms and their nearest-neighbor Be atoms (d_{O-Be}), are listed in Table 1. It can be clearly seen that, firstly, all the TM–O bond lengths (d_{TM-O}) in the 3d TM-doped (5,5) and (8,0) BeONTs are longer than the O–Be bond lengths of 1.615 Å and 1.660 Å in pristine (5,5) and (8,0) BeONTs respectively because the ionic radii of these 3d TM atoms are larger than that of the substituted Be atom. Secondly, the bond lengths between the three nearest-neighbor O atoms and their nearest-neighbor Be atoms (d_{O-Be}) around the 3d TM impurity in the 3d TM-doped (5,5) and (8,0) BeONTs are different from the O–Be bond lengths in pristine (5,5) and (8,0) BeONTs, implying that the introduced TM impurity also changes the interaction between near O and Be atoms. These results show that there exists a structural distortion around the 3d TM impurity in the 3d TM-doped (5,5) and (8,0) BeONTs.

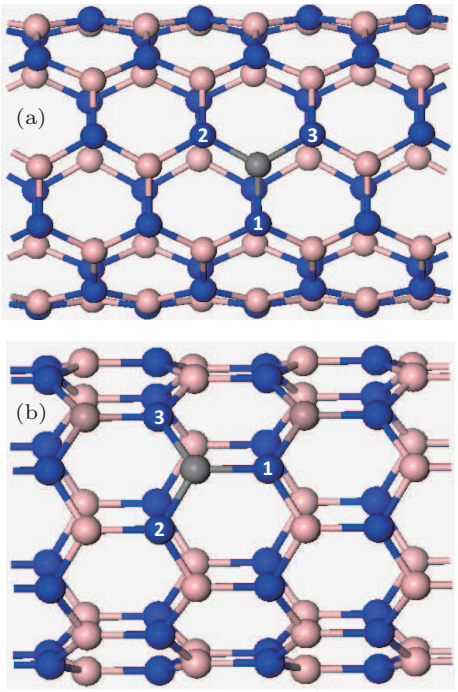


Fig. 1. (color online) Structure models of (a) TM-doped (5,5) BeONT and (b) TM-doped (8,0) BeONT, where the blue, yellow, and gray balls denote O, Be, and TM atoms, respectively. The blue balls marked with white numbers 1, 2, and 3 denote the three nearest-neighbor O atoms of the TM impurity.

The calculated magnetic moments of the TM-doped systems and the TM impurities (in parentheses) are listed in Table 1 for the 3d TM-doped (5,5) and (8,0) BeONTs. The magnetic moments of the TM-doped systems are contributed mainly by the TM impurities. Understandably, because the ground states of the pristine BeONTs are nonmagnetic, the magnetic moments of the TM-doped BeONTs should originate from the doped TM impurities. In Fig. 2, we plot the calculated magnetic moments of the 3d TM-doped (5,5) and (8,0) BeONTs versus the atomic numbers of the seven 3d TM impurities. Interestingly, the magnetic moments and their variation trends versus the atomic number are nearly identical for the 3d TM-doped (5,5) and (8,0) BeONTs. The magnetic moment increases for V- and Cr-doped BeONTs and reaches a maximum for Mn-doped BeONT ($4.43\mu_B$ and $4.44\mu_B$ for Mn-

doped (5,5) and (8,0) BeONTs, respectively), and then decreases for Fe-, Co-, Ni-, and Cu-doped BeONTs with further increasing atomic number. This is because the TM atom substituting for a cation (Be) in pristine (5,5) or (8,0) BeONT contributes two electrons to the anion (O). This results in the doped ions having $3d^3$, $3d^4$, $3d^5$, $3d^6$, $3d^7$, $3d^8$, and $3d^9$ electronic configurations for V^{2+}, Cr^{2+}, Mn^{2+}, Fe^{2+}, Co^{2+}, Ni^{2+}, and Cu^{2+}, respectively. These remaining d electrons are localized on the doped TM atoms and are mainly responsible for the magnetic moments of the TM-doped BeONTs.

Table 1. Calculated local bond lengths around substitutional 3d TM impurities, including bond lengths between the TM atoms and their nearest-neighbor O atoms (d_{TM-O1}, $d_{TM-O2} = d_{TM-O3}$) as well as the ranges of the bond lengths between the three nearest-neighbor O atoms and their nearest-neighbor Be atoms (d_{O-Be}), the magnetic moments μ of the TM-doped systems and the TM impurities (in parentheses) for 3d TM-doped (5,5) and (8,0) BeONTs.

Type	TM	d_{TM-O1}/Å	($d_{TM-O2} = d_{TM-O3}$)/Å	d_{O-Be}/Å	μ/μ_B
(5,5) BeONT	V	1.965	2.014	1.513–1.691	2.35 (2.30)
	Cr	1.973	1.990	1.514–1.675	3.37 (3.29)
	Mn	2.003	1.992	1.535–1.668	4.43 (4.17)
	Fe	1.925	1.952	1.536–1.686	3.79 (3.47)
	Co	1.926	1.962	1.525–1.681	2.84 (2.51)
	Ni	1.875	1.918	1.514–1.683	1.86 (1.50)
	Cu	1.926	1.943	1.521–1.677	0.9 (0.57)
(8,0) BeONT	V	1.939	2.043	1.503–1.645	2.34 (2.27)
	Cr	2.000	1.981	1.547–1.668	3.35 (3.25)
	Mn	1.964	2.107	1.480–1.641	4.44 (4.20)
	Fe	1.963	1.943	1.568–1.692	3.74 (3.43)
	Co	1.931	1.934	1.579–1.689	2.82 (2.48)
	Ni	1.926	1.942	1.581–1.683	1.84 (1.48)
	Cu	1.961	1.925	1.556–1.687	0.87 (0.52)

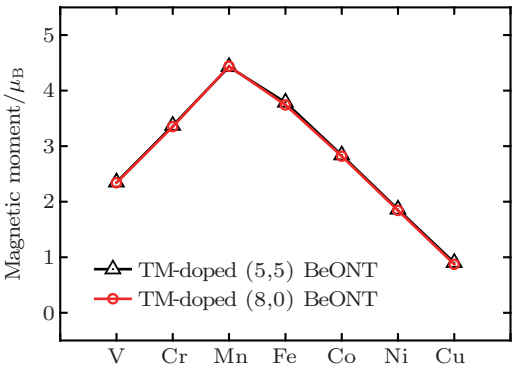


Fig. 2. (color online) Variations of the total magnetic moments of the 3d TM-doped (5,5) and (8,0) BeONTs with the atomic numbers of the seven 3d TM impurities.

The crystal field of the surrounding O ligands splits the five-fold degenerate d states of the free TM ion into two low-lying e_g orbitals (d_{z^2} and $d_{x^2-y^2}$) and three high-lying t_{2g} orbitals (d_{xy}, d_{xz}, and d_{yz}). According to Hund's rule, the detailed electronic configurations, the spin states on e_g and t_{2g} levels and the corresponding maximal net magnetic moments, are schematically shown in Fig. 3 for 3d TM ions at substitutional cation sites in II–VI DMSs. One can readily see that the maximal net magnetic moments are $3\mu_B$, $4\mu_B$, $5\mu_B$, $4\mu_B$, $3\mu_B$, $2\mu_B$, and $1\mu_B$ for V, Cr, Mn, Fe, Co, Ni, and Cu ions, respectively, consistent with the variation trend in Fig. 2 for the 3d TM-doped (5,5) and (8,0) BeONTs. The calculated magnetic moments are smaller than the predicted values of Hund's rule due to the strong hybridization between the 2p orbitals of the near O and Be atoms of BeONTs and the 3d orbitals of the TM ions.

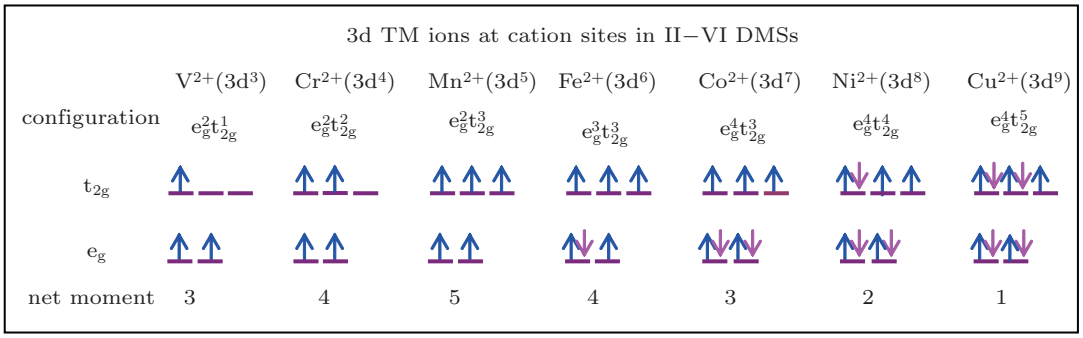


Fig. 3. (color online) Electronic configurations, spin states on t_{2g} and e_g levels, and the corresponding maximal net magnetic moments for 3d TM ions at substitutional cation sites in II–VI DMSs.

A better insight into the distribution of the electrons with energy can be gained from an analysis of the electronic density of states (DOS). So the total DOS with the black (red) lines representing the majority (minority) spins are shown in Figs. 4 and 5. The Fermi level is set at zero energy and indicated by the vertical blue dashed lines. From the total DOS of the pristine BeONTs, we can see that the pristine BeONTs are wide-band-gap nonmagnetic dielectrics because there is no spin polarization around the Fermi level which is just crossing the gap between the valence and the conduction bands. However, the asymmetry DOS near the Fermi level are obtained between majority and minority spins for all 3d TM-doped (5,5) and (8,0) BeONTs, indicating that magnetic moments exist. For V-doped (5,5) and (8,0) BeONTs, the majority spin electronic state crosses the Fermi level, which indicates a metallic behavior, while the minority spin electronic state is a dielectric because there is a large energy gap around the Fermi level. For Co- and Ni-doped (5,5) and (8,0) BeONTs, on the contrary, the minority spin electronic state crosses the Fermi level, while the majority spin electronic state has an energy gap around the Fermi level. Therefore, V-, Co-, and Ni-doped (5,5) and (8,0) BeONTs may have a half-metal ferromagnetism with 100% spin polarization and be good candidates for spintronic applications. It should be mentioned that for the materials with the metallicity in the majority spin electronic state and a dielectric in the minority spin electronic state, the half-metal ferromagnetism is presented, while for the materials with the metallicity in the minority spin electronic state and a dielectric in the majority spin electronic state, the metallicity may be influenced by their less density of the minority spin electronic state. An experimental investigation is needed for the half-metal ferromagnetism of the V-, Co-, and Ni-doped (5,5) and (8,0) BeONTs.

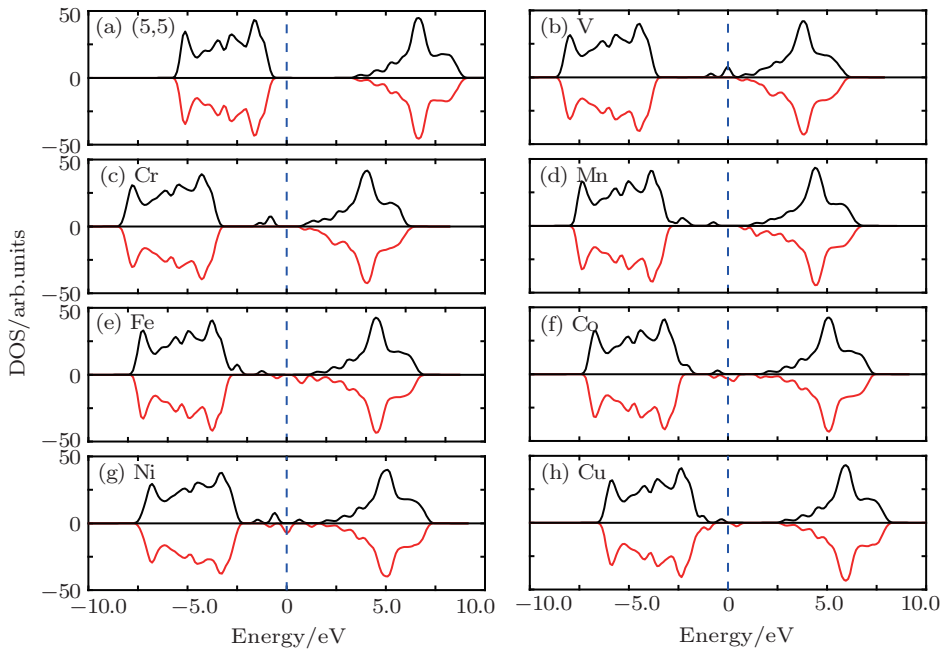


Fig. 4. (color online) Total density of states (DOS) with the black (red) line representing the majority (minority) spin for (a) pristine (5,5), (b) V-, (c) Cr-, (d) Mn-, (e) Fe-, (f) Co-, (g) Ni-, and (h) Cu-doped (5,5) BeONTs. The Fermi level is set at zero energy and indicated by the vertical blue dashed lines.

As is well known, in half-metal ferromagnets, the number of electrons in one spin channel is an integer. Since the total number of the valence electrons is an integer, it follows that the numbers of electrons in both spin channels are integers and so is their difference, and hence the integer spin magnetic moment. But from Table 1 we can see that the calculated magnetic moments of $2.35\mu_B$ ($2.30\mu_B$), $2.84\mu_B$ ($2.51\mu_B$), and $1.86\mu_B$ ($1.50\mu_B$) for V-, Co-, and Ni-doped (5,5) BeONTs (TM ions) as well as $2.34\mu_B$ ($2.27\mu_B$), $2.82\mu_B$ ($2.48\mu_B$), and $1.84\mu_B$ ($1.48\mu_B$) for V-, Co-, and Ni-doped (8,0) BeONTs (TM ions) are not integers and smaller than the maximal net magnetic moments of $3\mu_B$, $3\mu_B$, and $2\mu_B$ (see Fig. 3) for $V^{2+}(3d^3)$, $Co^{2+}(3d^7)$, and $Ni^{2+}(3d^8)$ ions respectively predicted by Hund's rule. To explain this inconsistency, the partial densities of states (PDOS) projected onto the TM atom (3d) as well as its nearest-neighbor O atom (2p) and next nearest-neighbor Be atom (2p) are presented in Fig. 6. It can be seen that the spin splitting mainly comes from TM (V, Co, and Ni) 3d, O 2p, and Be 2p states, and the TM (V, Co, and Ni) 3d states are hybridized with the nearest-neighbor O 2p states

and the next nearest-neighbor Be 2p states. This is one reason to reduce the magnetic moments of V, Co, and Ni ions in (5,5) and (8,0) BeONTs. Furthermore, the O and Be atoms around the 3d TM impurity, i.e. the nearest-neighbor O atom and the next nearest-neighbor Be atom, are polarized, while the other O and Be atoms are not polarized. That is to say, the polarizations are decided by the distance between the O (or Be) atom and the TM atom.

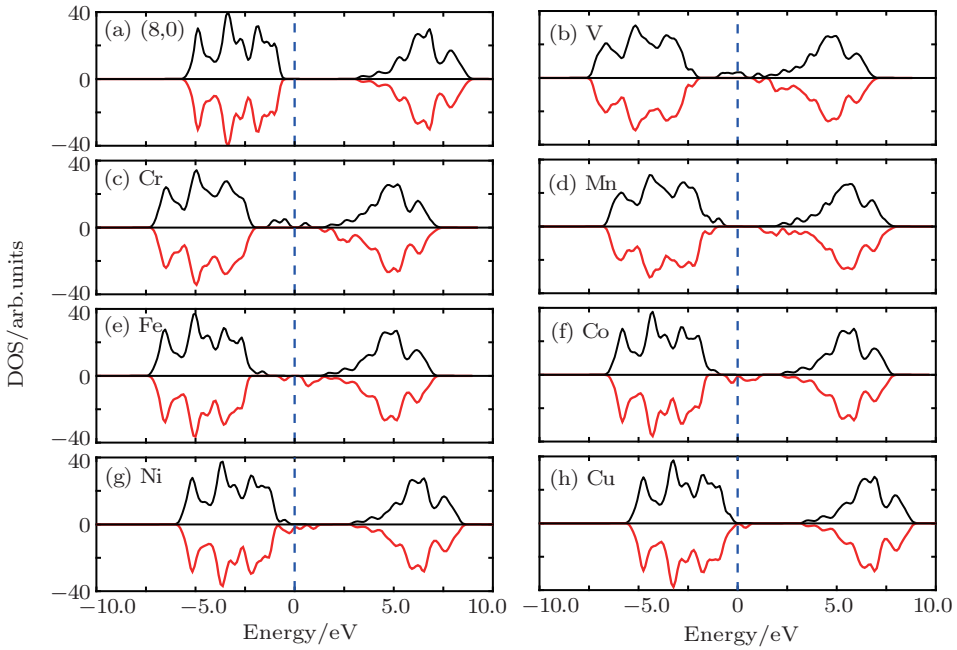


Fig. 5. (color online) Total density of states (DOS) with the black (red) line representing the majority (minority) spin for (a) pristine (8,0), (b) V-, (c) Cr-, (d) Mn-, (e) Fe-, (f) Co-, (g) Ni-, and (h) Cu-doped (8,0) BeONTs. The Fermi level is set at zero energy and indicated by the vertical blue dashed lines.

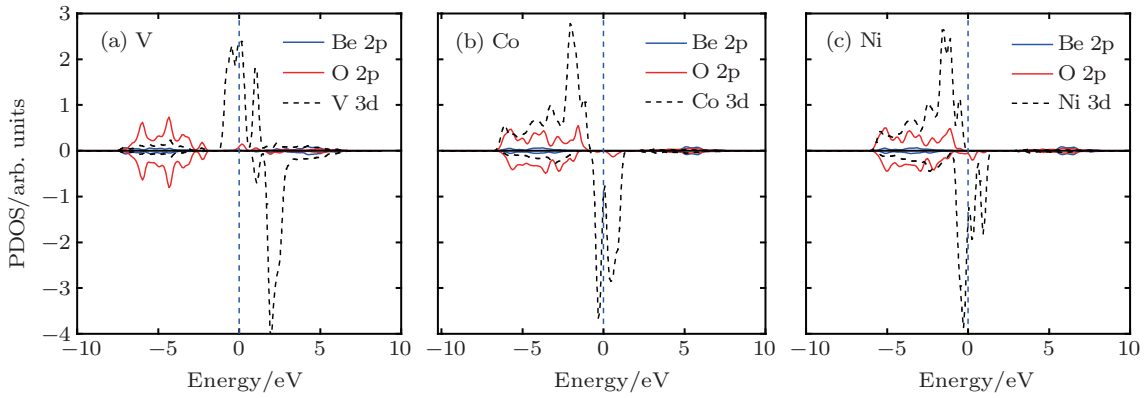


Fig. 6. (color online) Partial densities of states (PDOS) projected onto the TM atom (3d) as well as its nearest-neighbor O atom (2p) and next nearest-neighbor Be atom (2p) in (a) V-, (b) Co-, and (c) Ni-doped (8,0) BeONTs. The Fermi level is set at zero energy and indicated by vertical blue dashed lines.

4. Conclusions

In conclusion, the structural, electronic, and magnetic properties of seven 3d TM (V, Cr, Mn, Fe, Co, Ni, and Cu) doped (5,5) and (8,0) BeONTs have been investigated by using the PAW potential within DFT under GGA. The optimized structures show that the TM atom substituting a cation Be induces a structural distortion around the 3d TM impurity with respect to the pristine BeONT. The analysis of the DOS shows that the pristine (5,5) and (8,0) BeONTs are wide band gap nonmagnetic dielectrics, but asymmetry DOS near the Fermi level are obtained between majority and minority spins for all 3d TM-doped (5,5) and (8,0) BeONTs, and the magnetic moments of these TM-doped BeONTs mainly originate from the doped 3d TM impurities. The magnetic moments and their variation trends versus the atomic number are nearly identical for the 3d TM-doped (5,5) and (8,0) BeONTs, implying that they are independent of the tube chirality. The magnetic

moment increases for V- and Cr- doped BeONTs and reaches a maximum for Mn-doped BeONTs, and then decreases for Fe-, Co-, Ni-, and Cu-doped BeONTs successively, consistent with the predicted trend of Hund's rule to maximize the magnetic moments of the doped 3d TM ions. The magnetic moments are smaller than the predicted values of Hund's rule due to the strong hybridization between the p orbitals of the O and Be atoms of the BeONTs and the d orbitals of the TM ions. Interestingly, the V-, Co-, and Ni-doped (5,5) and (8,0) BeONTs with half-metal ferromagnetism and thus 100% spin-polarization character seem to be good candidates for spintronic applications.

References

[1] de Groot R A, Mueller F M, van Engen P G and Buschow K H J 1983 *Phys. Rev. Lett.* **50** 2024
[2] Kämper K P, Schmitt W, Güntherodt G, Gambino R J and Ruf R 1987 *Phys. Rev. Lett.* **59** 2788
[3] Watts S M, Wirth S, von Molnár, Barry A and Coey J M D 2000 *Phys. Rev. B* **61** 9621
[4] Tan M Q and Tao X M 1999 *Chin. Phys. Lett.* **16** 199
[5] Ishida S, Masaki T, Fujii S and Asano S 1998 *Physica B* **245** 1
[6] Picozzi S, Continenza A and Freeman A J 2002 *Phys. Rev. B* **66** 094421
[7] Kobayashi K I, Kimura T, Sawada H, Terakura K and Tokura Y 1998 *Nature* **395** 677
[8] Akinaga H, Manago T and Shirai M 2000 *Jpn. J. Appl. Phys.* **39** L1118
[9] Ohno H 1998 *Science* **281** 951
[10] Ueda K, Tabata H and Kawai T 2001 *Appl. Phys. Lett.* **79** 988
[11] Munekata H, Ohno H, von Molnar S, Segmüller A, Chang L L and Esaki L 1989 *Phys. Rev. Lett.* **63** 1849
[12] Kitchen D, Richardella A, Tang J M, Flatté M E and Yazdani A 2006 *Nature* **442** 436
[13] Sorokin P B, Fedorov A S and Chernozatonskii L A 2006 *Phys. Solid State* **48** 398
[14] Baumeier B, Krüger P and Pollmann J 2007 *Phys. Rev. B* **76** 085407
[15] Kresse G and Joubert D 1999 *Phys. Rev. B* **59** 1758
[16] Kresse G and Hafner J 1993 *Phys. Rev. B* **47** 558
[17] Kresse G and Hafner J 1994 *Phys. Rev. B* **49** 14251
[18] Kresse G and Furthmüller J 1996 *Comput. Mater. Sci.* **6** 15
[19] Kresse G and Furthmüller J 1996 *Phys. Rev. B* **54** 11169
[20] Perdew J P, Burke K and Ernzerhof M 1996 *Phys. Rev. Lett.* **77** 3865
[21] Monkhorst H J and Pack J D 1976 *Phys. Rev. B* **13** 5188
[22] Alam K M and Ray A K 2008 *Phys. Rev. B* **77** 035436
[23] Baumeier B, Krüger P and Pollmann J 2007 *Phys. Rev. B* **76** 085407